Simulation on Electrical Field Generation by Hall Effect in No-Insulation REBCO Pancake Coils

So Noguchi, Kwangmin Kim, and Seungyong Hahn

***Abstract*—The no-insulation (NI) winding technique is one of the most promising high-temperature superconducting (HTS) coil protection methods to realize the practical use of HTS magnets. Many NI $REBa_2Cu_3O_{7-x}$ (REBCO, RE = Rare Earth) magnets have been developed to generate ultrahigh magnetic fields for NMR or MRI magnets. When NI REBCO magnets are operated in a high magnetic field, uncommon phenomena can be observed, because the NI REBCO magnets have multicomplicated current paths. An unexpected voltage rise was experimentally observed during charging NI coils or after quench. The cause of such a voltage rise cannot be explained by means of a partial element equivalent circuit method, which was proposed to clarify such complicated current behavior. We think one of causes is an electric field generation by Hall effect. In this paper, therefore, we will investigate the electrical field behavior of NI REBCO coils by Hall effect. An unforeseen voltage would appear between terminals.**

***Index Terms*—Hall effect, high magnetic field magnets, no-insulation REBCO coils, quench analysis.**

I. Introduction

Ultra high magnetic field has been applied to NMR, MRI, and accelerator applications. $REBa_2\ Cu_3\ O_{7-x}$ (REBCO, RE = Rare Earth) coils are indispensable to generate such ultra high magnetic fields. A REBCO coil protection is one of serious problems in practical applications. The No-Insulation (NI) winding technique proposed by Hahn *et al.* [1] is a solution to escape REBCO magnets from burning-out after quench. The NI winding technique has greatly enhanced the thermal stability of REBCO magnets, as shown in experiments [1]–[3] and simulations [4], [5].

When an NI REBCO pancake coil transitions into a normal state, an operating current radially bypasses between terminal joints across winding turns. The bypassing current enhances the thermal stability of NI REBCO pancake coils, and it avoids the coils from burning-out, often called "*self-protecting*." However, since the bypassing current flows in a high magnetic field, there is a possibility that an expected electrical field is generated in the circumferential direction, according to the Hall effect [6], [7].

The electrical field generated by the Hall effect is linearly proportional to a current density and a magnetic field. The radial bypassing current flows through the stabilizer edges of REBCO tape [8] so that the current density in the radial direction increases under a high magnetic field of the axis direction. Consequently, a high electrical field is generated along the REBCO tape winding. When an NI REBCO magnet is operated under a high background field, the electrical Hall-effect field would be not negligible. Therefore, we try to estimate the electrical Hall-effect field in simulations.

In this paper, we focus on a voltage rise during charging NI double pancake coils. If the coil inductance and the contact resistance between turns are constant, the voltage must be constant. Indeed, a slight rise in voltage was observed in experiments. It may be caused by the change of coil inductance or the contact resistance. However, we try to explain it by Hall effect in simulations. The Hall voltages are estimated during charging NI REBCO double pancake coils, and the Hall voltage after quench is also shown.

II. Voltage Rise by Hall Effect

A. Hall Effect on NI REBCO Pancake Coils

When a large amount of current flows in a high magnetic field, charge carriers receive electromagnetic force, and it makes a voltage difference. This phenomenon is well known as the Hall effect, and it is expressed by the following equation [9]:

$$\boldsymbol{E}_{\mathrm{H}} = -R_{\mathrm{H}}\boldsymbol{J} \times \boldsymbol{B} \tag{1}$$

where $\boldsymbol{E}_{\mathrm{H}}$ is the electrical field caused by the Hall effect, R_{H} is the Hall coefficient, $\boldsymbol{J}$ is the current density, and $\boldsymbol{B}$ is the magnetic flux density, respectively.

Some current carries from turn to turn during charging or after quenching, as a radial current, because there is no insulation between turns. The radial current flows through stabilizers at the top and bottom edges of REBCO tapes, as shown in Fig. 1. That is, the radial current concentrates into the 5–20-μm-thick stabilizers [8], where the current density is extremely high.

Manuscript received August 29, 2017; accepted January 18, 2018. Date of publication January 30, 2018; date of current version February 15, 2018. This work was supported in part by JSPS KAKENHI under Grant 15KK0192. *(Corresponding author: So Noguchi.)*

S. Noguchi was with the National High Magnetic Field Laboratory, Florida State University, Tallahassee, FL 32310 USA. He is now with the Graduate School of Information Science and Technology, Hokkaido University, Sapporo 060-0814, Japan, and also with the Plasma Fusion and Science Center, Massachusetts Institute of Technology, Cambridge, MA 02138 USA (e-mail: noguchi@ssi.ist.hokudai.ac.jp).

K. Kim is with the National High Magnetic Field Laboratory, Florida State University, Tallahassee, FL 32310 USA.

S. Hahn was with the National High Magnetic Field Laboratory, Florida State University, Tallahassee, FL 32310 USA. He is now with the Department of Electrical and Computer Engineering, Seoul National University, Seoul 08826, South Korea.

Color versions of one or more of the figures in this paper are available online at http://ieeexplore.ieee.org.

Digital Object Identifier 10.1109/TASC.2018.2799573

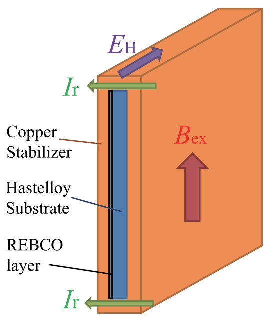

Fig. 1. Radial bypassing currents (I_r) flow into copper stabilizer on the top and bottom edges of REBCO tape. The Hall electrical field (E_H) is generated along tape-longitudinal direction under a high magnetic field (B_{ex}).

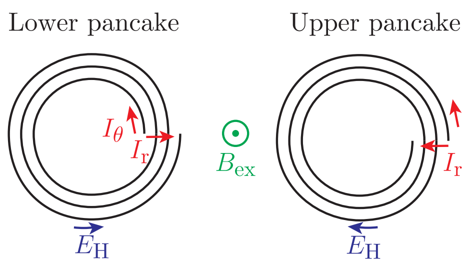

Fig. 2. For a double pancake coil, the circumferential current flows in the same direction, but the radial current in the opposite direction. Therefore, the Hall voltages in the opposite direction appear between upper and lower pancake coils.

When the radial current I_r passes through the REBCO tape edges, the current density J_r is given by

$$J_r = \frac{I_r}{2\pi r \times 2d} \quad (2)$$

where r and d are the coil radius and the stabilizer thickness of REBCO tape edge, respectively. The voltage difference of REBCO single pancake coil V_H is obtained from (1) and (2):

$$V_H = \int \boldsymbol{E}_H \cdot \mathrm{d}\boldsymbol{l} = -R_H \frac{I_r}{2d} B N_t \quad (3)$$

where $\boldsymbol{l}$ and N_t are, respectively, the length of REBCO tape and the number of turns.

B. Hall Voltage on NI REBCO Double Pancake Coil

For NI REBCO double pancake coils, since the upper and lower pancake coils are winding in the opposite direction each other, the radial currents on both the coils flow in the opposite direction during charging or bypassing. As seen in Fig. 2, the Hall electrical fields in the counter direction are generated on the upper and lower pancake coils. Consequently, the following equations are derived.

For upper pancake coil:

$$V_{\mathrm{coil,u}} = L_u \frac{\mathrm{d}I_{\theta,u}}{\mathrm{d}t} + M \frac{\mathrm{d}I_{\theta,l}}{\mathrm{d}t} + R_{t,u} I_{\theta,u} - V_{H,u} = R_{c,u} I_{r,u} \quad (4)$$

For lower pancake coil:

$$V_{\mathrm{coil,l}} = L_l \frac{\mathrm{d}I_{\theta,l}}{\mathrm{d}t} + M \frac{\mathrm{d}I_{\theta,u}}{\mathrm{d}t} + R_{t,l} I_{\theta,l} + V_{H,l} = R_{c,l} I_{r,l} \quad (5)$$

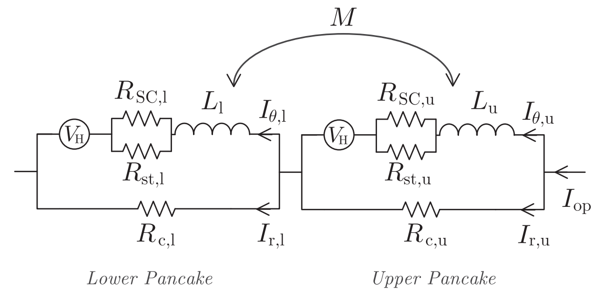

Fig. 3. Equivalent circuit for a double pancake coil to take into account the Hall voltage.

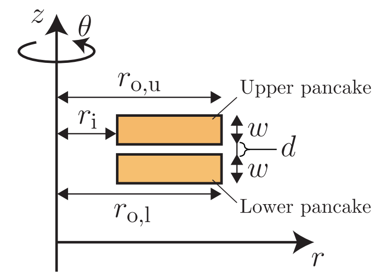

Fig. 4. Schematic view of double pancake coil with parameters.

where V_{coil}, L, M, R_t, R_c, and I_θ are the coil voltage, the self inductance, the mutual inductance, the composite resistance of REBCO layer and stabilizer, the contact resistance (sometimes called the characteristic resistance), and the circumferential current, respectively, and the subscript 'u' and 'l' mean the upper and lower pancake coils. Fig. 3 shows the equivalent circuit for NI REBCO double pancake coil as shown in Fig. 2. Here, the composite resistance R_t is given by

$$R_t = \left(R_{SC}^{-1} + R_{st}^{-1}\right)^{-1} \quad (6)$$

$$R_{SC} = \frac{E_c \ell}{I_\theta} \left(\frac{I_\theta}{I_c(B,\phi)}\right)^n \quad (7)$$

where R_{SC}, R_{st}, E_c, ℓ, I_c, B, ϕ and n are, respectively, the resistance of REBCO layer and stabilizer, the electrical-field criteria (1 μV/cm), the tape length of coil, the critical current, the magnetic field, its angle to the tape surface, and the power index. In this paper, the n-power law is employed, and the critical current I_c is obtained from the equation presented in [10].

III. Charging Simulation Results

To verify the Hall voltage, we compare the simulated voltage with the measurements of two different NI REBCO double pancake coils (DPs 1 and 2). In this paper, the Hall coefficient of copper R_H is 0.55×10^{-10} Ωm/T [11]. The thickness of copper stabilizer is 5 μm, and the coil is operated in a bath of liquid nitrogen.

A. Charging Simulation on DP 1

Fig. 4 shows the schematic drawing of double pancake coil with the parameters. Table I lists the specifications of DP 1, and Table II shows the circuit parameter of DP 1, respectively. The DP 1 was charged up to 54 A at a rate of 0.1 A/s in experiment.

TABLE I
SPECIFICATIONS OF DP 1

Inner radius r_{i} (mm)	30.93
Outer radius of upper pancake $r_{\mathrm{o,u}}$ (mm)	57.53
Outer radius of lower pancake $r_{\mathrm{o,l}}$ (mm)	57.51
Tape width w (mm)	4.1
Space between pancakes d (mm)	0.14
No. of upper pancake (turn)	218
No. of lower pancake (turn)	217
Coil critical current (A)	53.7
Coil inductance (mH) (measured)	18.87
Characteristic resistance (mΩ) (measured)	2.6

TABLE II
CIRCUIT PARAMETERS OF DP 1

Inductance of upper pancake L_{u} (mH)	5.17
Inductance of lower pancake L_{l} (mm)	5.21
Mutual inductance M (mH)	4.48
Contact resistivity ($\mu\Omega\cdot\mathrm{cm}^2$)	65.5
Characteristic resistance of upper pancake $R_{\mathrm{c,u}}$ (m Ω)	1.31
Characteristic resistance of lower pancake $R_{\mathrm{c,l}}$ (m Ω)	1.30
Current sweep ratio (A/s)	0.1

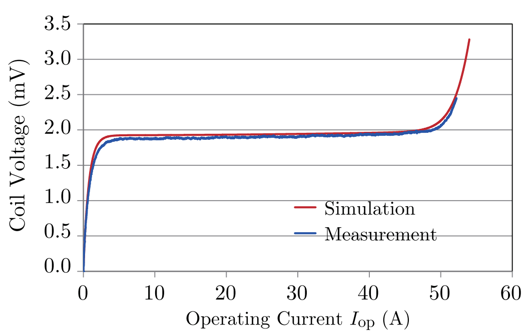

Fig. 5. Measured and simulated V–I curve of DP 1.

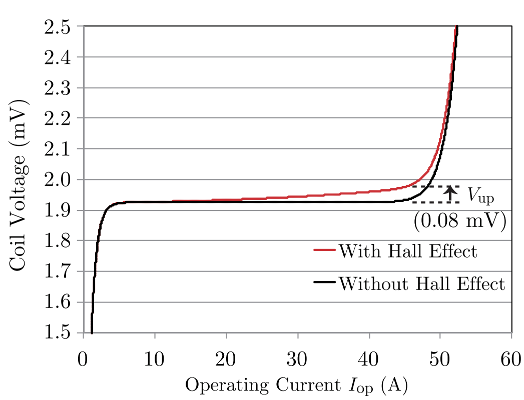

Fig. 6. Simulated V–I curves with and without Hall voltage in DP 1.

The measured V–I curve is shown in Fig. 5. Supposing that there is no Hall voltage rise, the voltage must be constant after the first large inductive voltage rise. However, the gradual voltage rise of 0.09 mV was observed after the voltage went up to approximately 1.8 mV.

The simulation result is also shown in Fig. 5. We can see the good agreement between the measurement and the simulation. Fig. 6 shows the simulation result without considering the Hall voltage. The voltage rise V_{up} of 0.08 mV can be seen from Fig. 6. It is very close to the measured voltage rise of 0.09 mV.

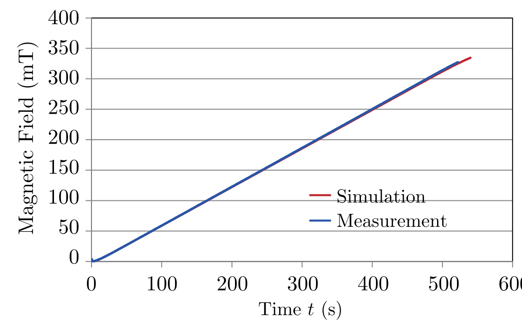

Fig. 7. Measured and simulated axial field as function of time in DP 1.

TABLE III
SPECIFICATIONS OF DP 2

Inner radius r_{i} (mm)	28.90
Outer radius of upper pancake $r_{\mathrm{o,u}}$ (mm)	57.45
Outer radius of lower pancake $r_{\mathrm{o,l}}$ (mm)	57.39
Tape width w (mm)	7.1
Space between pancakes d (mm)	0.14
No. of upper pancake (turn)	238
No. of lower pancake (turn)	236
Coil critical current (A)	62.6
Coil inductance (mH) (measured)	18.93
Characteristic resistance (mΩ) (measured)	2.5

TABLE IV
CIRCUIT PARAMETERS OF DP 2

Inductance of upper pancake L_{u} (mH)	5.52
Inductance of lower pancake L_{l} (mm)	5.43
Mutual inductance M (mH)	4.42
Contact resistivity ($\mu\Omega\cdot\mathrm{cm}^2$)	67.5
Characteristic resistance of upper pancake $R_{\mathrm{c,u}}$ (m Ω)	0.87
Characteristic resistance of lower pancake $R_{\mathrm{c,l}}$ (m Ω)	0.86
Current sweep ratio (A/s)	0.1

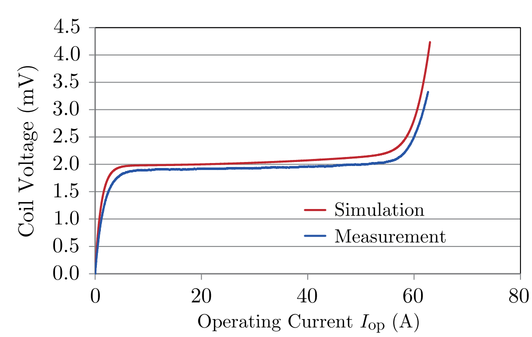

Fig. 8. Measured and simulated V–I curve of DP 2.

Fig. 7 shows the measured and simulated axial magnetic fields at the magnet center. The simulation agrees with the measurement well.

B. Charging Simulation on DP 2

Tables III and IV list the specifications and circuit parameter of DP 2, respectively. The DP 2 went up to 63 A at a rate of 0.1 A/s. Fig. 8 shows the measured coil voltage V as a function

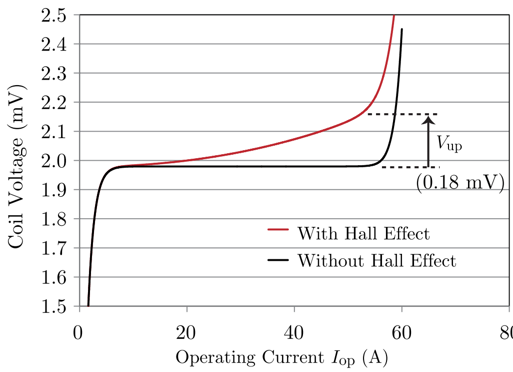

Fig. 9. Simulated V–I curves with and without Hall voltage in DP 2.

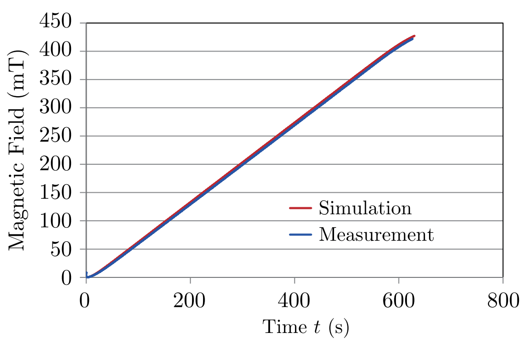

Fig. 10. Measured and simulated axial field as function of time in DP 2.

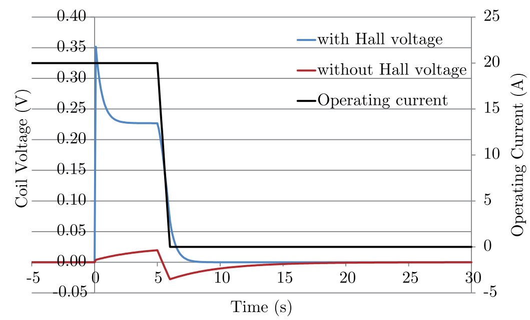

Fig. 11. Coil voltage in DP 1 initially operated at 20 A, and the lower pancake coil is transitioned into a normal state at $t = 0$ s. The operating current goes down to 0 in 1 s after the normal-state transition.

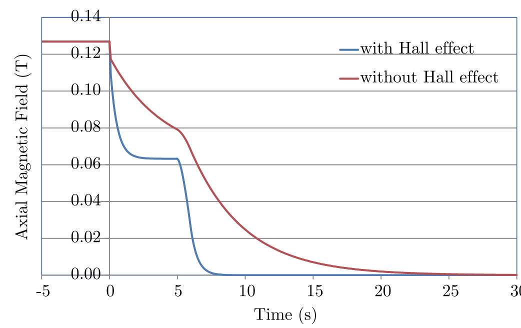

Fig. 12. Axial magnetic field generated in DP 1 after normal-state transition of lower pancake coil and during current shutdown.

of the coil current I_{op} together with the simulation result. The simulated coil voltage is slightly larger than the measured one, however the good agreement can be seen.

A voltage rise V_{up} of 0.17 mV was observed in the experiment, as can be seen in Fig. 8. The simulated coil voltage without considering Hall effect is shown in Fig. 9. Comparing with the results with/without the Hall effect, The simulated voltage rise V_{up} is 0.18 mV, which is very close to the experiment.

Fig. 10 shows the measured and simulated magnetic fields at the magnet center for DP 2. There is no difference between the experiment and the simulation.

IV. Quench Simulation Result

A. Hall Voltage Estimation

When the lower pancake coil of DP 1, which was operated in an external magnetic field of 10 T, transitioned into a normal state, a high Hall voltage would appear. All the operating current in the lower pancake coil carries through the edges of REBCO tape in the radial direction. The coil parameters are listed in Table I. It is supposed that the operating temperature is 20 K. According to (3), the Hall voltage is

$$\begin{aligned} V_{\mathrm{H},1} &= -0.55 \times 10^{-10} \times \frac{-20}{2 \times 5 \times 10^{-6}} \times 10 \times 217 \\ &= 0.239\, V. \end{aligned} \tag{8}$$

Since the contact resistance $R_{\mathrm{ct},1}$ is 1.30 mΩ shown in Table II, the radial resistive voltage is 0.026 V ($= I_{\mathrm{r},1} \times R_{\mathrm{ct},1} = 20$ A $\times$ 1.30 mΩ). The Hall voltage (0.239 V) is much higher than the radial resistive voltage (0.026 V). Accordingly, a large Hall voltage of an NI REBCO insert coil would be observed after quench in a high external magnetic field generated by an outsert magnet.

B. Circuit Simulation After Normal-State Transition

The Hall voltage is roughly estimated using (3) in the above section. Next, the coil voltage is simulated with the equivalent circuit as shown in Fig. 3. As the simulation condition, the normal-station transition of lower pancake coils in DP 1 occurs at $t = 0$, when the DP 1 magnet is operated at 20 A. At $t = 5$ s, the operating current decreases to 0 in 1 s.

Fig. 11 plots the coil voltage with/without the Hall voltage together with the operating current, as the equivalent circuit simulation result. The coil voltage considering the Hall voltage is completely different from that without Hall voltage. The simulated coil voltage is slightly higher than that of the above estimation. Fig. 12 shows the axial magnetic filed generated by DP 1 at the magnet center with/without the Hall effect. The profiles of the magnetic field are different each other. The magnetic field decay without Hall effect is slightly slow.

From the simulation results, the coil voltage unexpectedly rises up due to the Hall effect. When NI REBCO pancake coils operates in a high magnetic field, a countermeasure would be required against coil voltage rise after a normal-state transition.

V. Conclusion

When an NI REBCO pancake coil is charged or quenched, a radial current flows in the radial direction. An expected electrical field would be generated along coil winding, since the radial current flows in a high magnetic field. The measured voltage rise during charging NI REBCO pancake coils can be reproduced with the equivalent circuit simulation considering the Hall effect. In addition, an unexpected voltage rise of NI REBCO pancake coil is estimated after quench in a high magnetic field by the proposed equivalent circuit model. However, a voltage rise by Hall effect has not been confirmed in experiments. Therefore, we have to keep investigating the cause of the voltage rise, such as the change of coil inductance and contact resistance.

The equivalent circuit shown in this paper is modeled too simply, and not precisely. In fact, the Hall-effect field must appear on a small edge portion of REBCO tape. Therefore, we have to simulate the Hall-effect field using a finite element method in order to investigate more accurate behavior in NI coils.

REFERENCES

[1] S. Hahn, D. K. Park, J. Bascuñán, and Y. Iwasa, "HTS pancake coils without turn-to-turn insulation," *IEEE Trans. Appl. Supercond.*, vol. 21, no. 3, pp. 1592–1595, Jun. 2011.

[2] J. Song *et al.*, "Dynamic response of no-insulation and partial-insulation coils for HTS wind power generator," *IEEE Trans. Appl. Supercond.*, vol. 25, no. 3, Jun. 2015, Art. no. 5202905.

[3] S. Noguchi *et al.*, "Experiment and simulation of impregnated no-insulation REBCO pancake coil," *IEEE Trans. Appl. Supercond.*, vol. 26, no. 4, Jun. 2016, Art. no. 4601305.

[4] T. Wang *et al.*, "Analyses of transient behaviors of no-insulation REBCO pancake coils during sudden discharging and overcurrent," *IEEE Trans. Appl. Supercond.*, vol. 25, no. 3, Jun. 2015, Art. no. 4603409.

[5] Y. Wang, H. Song, W. Yuan, Z. Jin, and Z. Hong, "Ramping turn-to-turn loss and magnetization loss of a no-insulation (RE)Ba2Cu3Ox high temperature superconductor pancake coil," *J. Appl. Phys.*, vol. 121, 2017, Art. no. 113903.

[6] X. Huang and Y. M. Eyssa, "Stability of large current aluminium stabilized conductors," *Cryogenics*, vol. 32, no. 1, pp. 28–34, 1992.

[7] T. Tsuchiya, S. Noguchi, H. Yamashita, A. Ishiyama, N. Yanagi, and T. Mito, "Transient Stability analysis of large aluminum stabilized superconductor by 2D and 3D finite element analysis," *IEEE Trans. Appl. Supercond.*, vol. 14, no. 2, pp. 1330–1333, Jun. 2004.

[8] S. Noguchi, K. Monma, H. Igarashi, and A. Ishiyama, "Investigation of current flow between turns of NI REBCO Pancake coil by 2-D finite-element method," *IEEE Trans. Appl. Supercond.*, vol. 26, no. 3, Apr. 2016, Art. no. 4901205.

[9] P. W. Eckels and J. H. Parker Jr., "The Hall effect in superconductor stability," *Cryogenics*, vol. 32, no. 5, pp. 490–493, 1992.

[10] H. Ueda *et al.*, "Numerical simulation on magnetic field generated by screening current in 10-T-class REBCO coil," *IEEE Trans. Appl. Supercond.*, vol. 26, no. 4, Jun. 2016, Art. no. 4701205.

[11] N. Yanagai *et al.*, "Experimental observation of anomalous magneto-resistivity in 10–20 kA class aluminum-stabilized superconductors for the large helical device," *Adv. Cryogenic Eng.*, vol. 40, pp. 459–467, 1994.